AGU PUBLICATIONS

JGR

Journal of Geophysical Research: Solid Earth

RESEARCH ARTICLE
10.1002/2015JB012742

Key Points:
- Identification of an error in published *ICE6G_C(VM5a)* radial velocity field
- Identification of an error in published *ICE6G_C(VM5a)* Stokes' coefficients
- Validation of viscoelastic Love number ratios of Purcell et al. (2011)

Supporting Information:
- Supporting Information S1
- Data Set S1
- Data Set S2

Correspondence to:
A. Purcell,
Anthony.Purcell@anu.edu.au

Citation:
Purcell, A., P. Tregoning, and A. Dehecq (2016), An assessment of the *ICE6G_C(VM5a)* glacial isostatic adjustment model, *J. Geophys. Res. Solid Earth*, *121*, 3939–3950, doi:10.1002/2015JB012742.

Received 14 DEC 2015
Accepted 31 MAR 2016
Accepted article online 4 APR 2016
Published online 21 MAY 2016

An assessment of the *ICE6G_C(VM5a)* glacial isostatic adjustment model

A. Purcell[1], P. Tregoning[1], and A. Dehecq[1,2]

[1]Research School of Earth Sciences, Australian National University, Canberra, ACT, Australia, [2]Polytech Annecy-Chambery, Annecy le Vieux, France

Abstract The recent release of the next-generation global ice history model, *ICE6G_C(VM5a)*, is likely to be of interest to a wide range of disciplines including oceanography (sea level studies), space gravity (mass balance studies), glaciology, and, of course, geodynamics (Earth rheology studies). In this paper we make an assessment of some aspects of the *ICE6G_C(VM5a)* model and show that the published present-day radial uplift rates are too high along the eastern side of the Antarctic Peninsula (by ~8.6 mm/yr) and beneath the Ross Ice Shelf (by ~5 mm/yr). Furthermore, the published spherical harmonic coefficients—which are meant to represent the dimensionless present-day changes due to glacial isostatic adjustment (GIA)—contain excessive power for degree ≥90, do not agree with physical expectations and do not represent accurately the *ICE6G_C(VM5a)* model. We show that the excessive power in the high-degree terms produces erroneous uplift rates when the empirical relationship of Purcell et al. (2011) is applied, but when correct Stokes coefficients are used, the empirical relationship produces excellent agreement with the fully rigorous computation of the radial velocity field, subject to the caveats first noted by Purcell et al. (2011). Using the Australian National University (ANU) groups *CALSEA* software package, we recompute the present-day GIA signal for the ice thickness history and Earth rheology used by Peltier et al. (2015) and provide dimensionless Stokes coefficients that can be used to correct satellite altimetry observations for GIA over oceans and by the space gravity community to separate GIA and present-day mass balance change signals. We denote the new data sets as *ICE6G_ANU*.

1. Introduction

It has long been recognized that the mathematical expressions for the gravitational and deformational effects of glacial isostatic adjustment (GIA) are almost identical, with the two terms having a fixed ratio for each spherical harmonic degree. For modern GIA effects the relationship is predominantly elastic and the constants of proportionality are negative: as surface mass is reduced/increased elastic uplift/subsidence occurs. For the paleo-GIA component the relationship is viscoelastic and the constants of proportionality are positive: uplift/subsidence results from the flow of mantle material to/from the region being observed. Comparison of gravitational and deformational components therefore has the potential to separate the paleo-GIA and modern GIA components which is of enormous significance in observations of the hydrosphere. In particular, the effect of seafloor subsidence on satellite altimetry observations of sea level and the impact of mantle flow on mass balance estimates from space gravity missions (e.g., Gravity Recovery and Climate Experiment (GRACE)) need to be removed to obtain an accurate understanding of the ice-ocean system.

The potential importance of this issue led *Purcell et al.* [2011] to determine viscoelastic ratios of proportionality as a function of degree that they suggested were independent of rheology and ice load history for epochs sufficiently removed from significant changes in load. The validity of this study was subsequently questioned in *Peltier et al.* [2015] and *Argus et al.* [2014] where the empirical relationship derived by *Purcell et al.* [2011] was applied to produce results strongly at variance with those presented for *ICE6G_C*.

ICE6G_C is a model of the changes in ice thickness of the major ice sheets through the Last Glacial Maximum (LGM) to the present and was described in *Argus et al.* [2014] and *Peltier et al.* [2015]. The corresponding model of the Earth's rheological structure was labeled VM5a. Both the ice and rheological models are refinements of earlier inversions, the most recent of which (ICE5G (VM2) [*Peltier*, 2004]) has been widely used to model ongoing glacio-hydro-isostatic effects.

Peltier et al. [2015] provided a spherical harmonic representation (in the form of Stokes' coefficients) of the present-day isostatic response of the Earth as predicted by their model which, in principle, can be used to remove the effects of this process from space gravity estimates of the Earth's temporal gravity field so that present-day mass balance changes can be determined. They further demonstrated that when the empirical relationship between geoid change and vertical deformation developed by *Purcell et al.* [2011] is applied to these coefficients the resulting function disagrees markedly from the uplift rates calculated for *ICE6G_C*. They concluded that "there is a highly significant error in the empirical prediction, irrespective of the resolution of the empirical solution employed," implying that accurate uplift rates can only be generated through the full computation of a GIA model. In this paper we explore the issue of why the empirical relationship derived by *Purcell et al.* [2011] did not produce accurate radial uplift rates in this application.

The comparison between the empirically and rigorously calculated uplift rates presented by *Peltier et al.* [2015] is based on a misapplication of the technique of *Purcell et al.* [2011]. However, applying the corrected Love number ratios for degree >60 does not explain the disagreement between the empirical approximation and the rigorously derived velocity field since the misfit is in fact amplified. There remain two possible explanations for this discrepancy

1. Despite *Purcell et al.*, 2011's [2011] claims that their derived viscoelastic Love number ratios are independent of load history and rheology, their empirical relationship does not hold for ice model *ICE6G_C*, rheological model VM5a, the particular combination *ICE6G_C(VM5a)* or simply does not hold, in general. This would make the technique inappropriate for any modeling purposes since uncertainties in ice load history and rheology remain significant.
2. There is some methodological error in the analysis of *Peltier et al.* [2015] and *Argus et al.* [2014] that produces the observed discrepancy between the velocity field and the empirical approximation.

To test each of these hypotheses, we applied the ANU group's *CALSEA* software *Lambeck et al.* [2003] to the inputs of the *ICE6G_C(VM5a)* model and compared the results of our calculations with the publicly available *ICE6G_C(VM5a)* radial velocity field (http://www.atmosp.physics.utoronto.ca/~peltier/data) and the Stokes' coefficients of *Peltier et al.* [2015]. Our analysis shows that neither the gridded uplift rates nor the spherical harmonic coefficients accurately represent the present-day GIA signal based on the *ICE6G_C(VM5a)* model. The published velocity field gives uplift rates that are demonstrably inaccurate and nonphysical in the Antarctic region, where the net change in load seems to have been miscalculated by *Peltier et al.* [2015]. Additionally, the radial velocity field and Stokes' coefficients supplied in *Peltier et al.* [2015] are inconsistent.

We reassess the accuracy of the empirical relation of *Purcell et al.* [2011] and find that it can reproduce fully rigorous uplift rate computations over continents with an accuracy of better than 1 mm/yr. We derive and provide spherical harmonic coefficients that accurately represent the *ICE6G_C(VM5a)* GIA signal and do not contain the erroneous unphysical components apparent in the originally published data. Our coefficients can be used to remove GIA effects from estimates of temporal gravity field such as those from the Gravity Climate and Recovery Experiment (GRACE) mission subject to the accuracy of the *ICE6G_C(VM5a)* model. Finally, we provide computed velocity fields for radial deformation and geoid change and for the *ICE6G_C(VM5a)* model may be applied without the need for any spatial filtering.

2. The *CALSEA* Software Package

The Earth's response to changes in surface load distribution resulting from mass exchanges between ice sheets and oceans has been the subject of mathematical and computational investigation over many decades. The seminal theoretical investigation of postglacial rebound and relative sea level change was by *Farrell and Clark* [1976] in which the governing integral equation for sea level change was derived. This type of analysis requires a number of model inputs that may be broadly separated into the ice load history (specified by changes in ice thickness as a function of position and time), Earth response parameters (in the form of an assumed rheological structure and a specific choice of parameter values), and ocean loading parameters (which are themselves functions of rebound, ice volume, ice distribution, and ocean geometry).

As computational resources continue to improve, a wider variety of potential rheological structures is being investigated through the use of finite volume and finite element analysis [e.g., *Paulson et al.*, 2005; *Wu and Van Der Wal*, 2003; *Dal Forno et al.*, 2005]. Nonetheless, the most widely used model for Earth response is that of a spherically symmetric, radially stratified Maxwell-viscoelastic body with an elastic (or effectively elastic)

lithosphere and a liquid core [e.g., *Tushingham and Peltier*, 1992; *Kendall et al.*, 2004]. For such a body the relaxation may be described through viscoelastic Love numbers by solving the Laplace-transformed governing equations derived by *Wu and Peltier* [1982] using the elastic structure given by *Dziewonski and Anderson* [1981] and inverting into the time domain using a Bromwich path integration [e.g., *Cambiotti and Sabadini*, 2010] or a collocation technique [e.g., *Mitrovica and Peltier*, 1991]. As discussed in this latter study, care must be taken that the choice of collocation points in the Laplace domain adequately represents the relaxation spectra of the rheology in question; otherwise, the derived residuals may exhibit significant numerical instability. While more sophisticated rheological structures may be considered, *Paulson et al.* [2007] and *Paulson and Richards* [2009] demonstrated that inversion of postglacial rebound observations have limited ability to resolve detailed viscosity structures. Nonetheless, it seems that data from different regions do exhibit different relaxation timescales (as demonstrated in *Nakada and Lambeck* [1989] and *Lambeck et al.* [1998]).

While *Farrell and Clark* [1976] considered deformational, gravitational, and volumetric mechanisms of sea level change, they neglected the effect of changes in the Earth's rotational moment of inertia due to mass redistribution across its surface and at depth. This process was analyzed by *Lambeck* [1980], *Sabadini and Peltier* [1981], *Yuen et al.* [1982], and *Wu and Peltier* [1984] who demonstrated its significance and essential character. In the course of these analyses the rotational feedback on sea level change was shown to be dominated by the spherical harmonic term of degree 2, order 1 and theory was developed for a Love number representation. The rotational term was further explored and refined by *Milne and Mitrovica* [1998], *Mound et al.* [2003], *Mitrovica et al.* [2005], and *Mitrovica and Wahr* [2011] with particular attention to the effect on estimates of GIA-induced true polar wander. In this analysis we have employed the rotational contribution for *ICE6G_C(VM5a)* calculated by Mitrovica, the corresponding geoid velocity corrections being $\dot{C}_{21}^{\mathrm{rot}} = -1.75 \times 10^{-9}$, $\dot{S}_{21}^{\mathrm{rot}} = 2.27 \times 10^{-}8$ (J. Mitrovica, personal communication).

The initial analysis of *Farrell and Clark* [1976] also neglected the effects of a time-varying ocean function, and their formulation implicitly assumed that ocean area and geometry would not change significantly. *Johnston* [1993], *Peltier* [1994], *Peltier* [1998], and *Milne* [1998] demonstrated that this assumption produced significant errors and that an accurate solution of the sea level equation required multiple iterations in which variations in ocean area and geometry due to rebound and changes in ice sheet grounding lines are calculated and incorporated.

The *CALSEA* software package obtains solutions to the sea level governing equation of *Farrell and Clark* [1976]. Originally, the theory was that employed in *Nakada and Lambeck* [1987] to which were added subsequent refinements to incorporate changes in ocean geometry [*Johnston*, 1993; *Lambeck et al.*, 2003] and the rotational component of *Wu and Peltier* [1984] (with later adjustments to incorporate the corrections of *Mitrovica et al.* [2005] and *Mitrovica and Wahr* [2011]). The validity of the code and the algorithms employed has been investigated in *Mitrovica* [2003] and *Mitrovica and Milne* [2003] who concluded that the underlying methodology is accurate. Calculations of velocity fields and changes in relative sea level derived using the *CALSEA* packages have reproduced the detailed behavior of a wide variety of observational data sets in the near, far, and intermediate fields on a variety of time scales [see, e.g., *Lambeck and Purcell*, 2005; *Lambeck et al.*, 2006, 2010, 2014].

3. *ICE6G_C(VM5a)* Model Results

3.1. Near-Field Radial Uplift

We denote the modern radial velocity field for *ICE6G_C(VM5a)* published by *Peltier et al.* [2015] as VF1 and that derived by applying the *CALSEA* code to *ICE6G_C(VM5a)* as VF2. The difference VF1 − VF2 is shown in Figure 1. In the far field the disagreement between the two data sets is dominated by a degree 2 order 1 term, reflecting a minor discrepancy in the calculation of the rotational term, but the amplitude of this component is less than 0.2 mm/yr, and we do not describe it any further. In the near field of the former ice sheets the disagreement between VF1 and VF2 is more marked. Over Fennoscandia the magnitude of the discrepancy between the two varies from −2.2 mm/year to 1.4 mm/yr. The corresponding difference in amplitude over North America ranges from −2.2 mm/yr to 2.2 mm/yr. In all regions there are discrepancies that follow the geometry of coasts and continental shelves. In the near field there are significant differences in uplift rates at points where ice loading has transitioned to water loading and at points that have lain below sea level during the deglaciation phase. We return to this point later. In the case of Antarctica, the disagreement between the two velocity fields is particularly marked, ranging from −1.5 to 8.6 mm/yr. As shown in Figure 2 the largest differences between

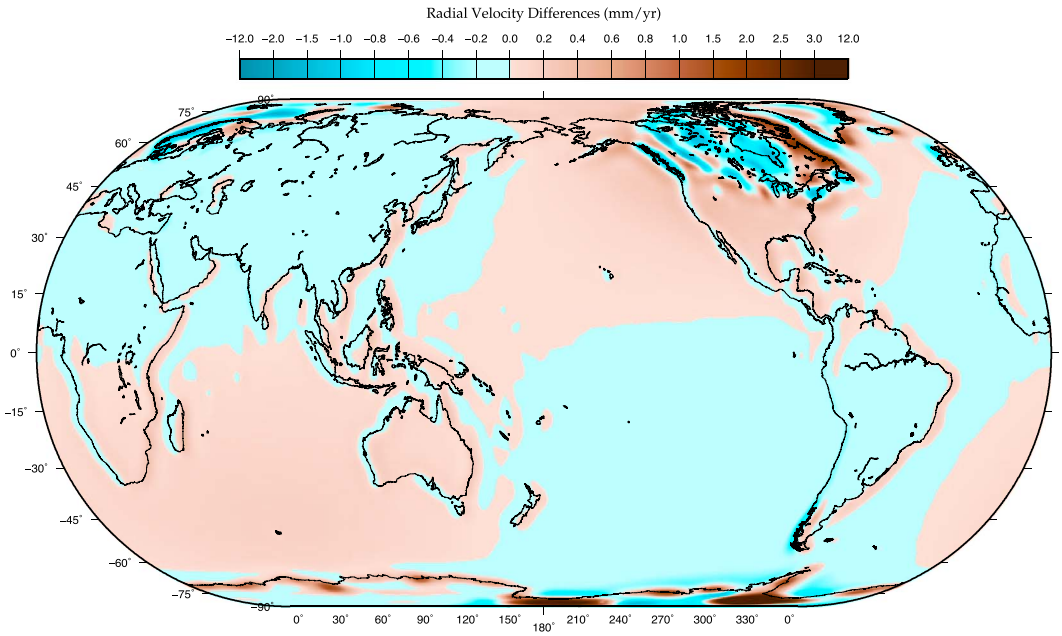

Figure 1. Illustration of the difference between the velocity field of *Peltier et al.* [2015] and that derived from *CALSEA*. The difference is dominated by a degree 2 order 1 signal of amplitude <0.2 mm/yr. Over Fennoscandia the discrepancy varies from −2.2 to 1.4 mm/yr. For North America the corresponding range is −2.2–2.2 mm/yr. The largest discrepency between the two velocity fields (−1.5–8.6 mm/yr) is observed over Antarctica.

the two sets of results occur over the ice shelves of the Weddell and Ross Seas where the VF1 uplift rate of *Argus et al.* [2014] is much larger than we obtain. That these discrepancies coincide so precisely with ice shelves suggests that there is some discrepancy between the two techniques used to calculate the progression of the loading function through time since these regions constitute the classic example of a retreating ice sheet being replaced by a water load. Such a discrepancy would also contribute to the differences in uplift rate observed over North America and Fennoscandia.

Figure 3 illustrates three possible unloading scenarios. In the first (a and b) the ice sheet remains grounded between the two time steps (that is, $\rho_i l(t) > \rho_w b(t)$, where ρ_i and ρ_w are the density of ice and water, respectively, l is ice thickness, and b is bathymetry or ocean depth). Thus, the change in load is simply the change in grounded ice thickness. In this case (shown in Figures 3a and 3b) the total change in load between the two time steps is $\rho_i(l(t_2) - l(t_1))$.

In the second case (Figures 3c and 3d) the ice load is initially thick enough that it is grounded ($\rho_i l(t_1) > \rho_w b(t_1)$), but as the ice thins, it becomes too small to displace the entire water column ($\rho_i l(t_2) < \rho_w b(t_2)$), and thus, the ice begins to float. At that point the local load corresponds not to ice thickness but to water depth. The net change in load between the two time steps is therefore $\rho_w b(t_2) - \rho_i l(t_1)$.

In the third case (Figures 3e and 3f) the ice sheet is never grounded and the total change in load at this location is simply $\rho_w(b(t_2) - b(t_1))$. We reconstruct paleotopography from modern topography using the relation $\mathrm{Topo}(t) = \mathrm{Topo}(\mathrm{present}) - \Delta\mathrm{RSL}(t)$ and bathymetry derived as $b(t) = \max(0, -\mathrm{Topo}(t))$.

This simple discussion illustrates two potential sources of inaccuracy in calculations of GIA that are familiar to those who model postglacial rebound but are not often treated explicitly and are consequently poorly understood by researchers in other fields:

1. The modern topographic data set used in GIA code should be both accurate and high resolution for calculations of the water load to be correct. In this context the *CALSEA* code uses the GEBCO_08 topographic database (version 20100927, http://www.gebco.net) for all points north of 60° south. South of this parallel topography and bathymetry are derived from the BEDMAP data sets [*Fretwell et al.*, 2013] using bathymetry for all points at which the modern ice is not grounded and ice surface elevation above sea level otherwise (see Figure 4). This combined topographic data set is sampled spatially at intervals of 3 min when calculating water loading and ocean volume in *CALSEA*.

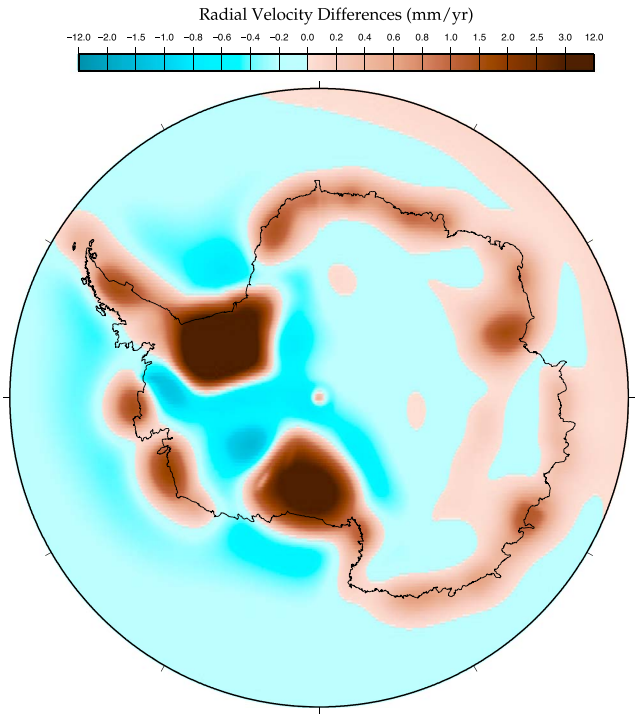

Figure 2. Illustration of the difference between the velocity field of *Peltier et al.* [2015] and that derived from *CALSEA* over Antarctica. The difference is largest over the Weddell and Ross Seas but generally follows the coastline and becomes significant at all points where transitions from ice loading to water loading have occurred during the Late Glacial and Holocene.

2. The ice sheet grounding line defines the point where ice loading transitions to water loading and must be accurately determined for each time step throughout the loading history. This operation requires multiple iterations of the governing equation (as discussed in *Johnston* [1993] and *Milne and Mitrovica* [1998]). The *CALSEA* code requires nine iterations to provide subcentimeter convergence at all points on the globe, five iterations are generally adequate for all regions except the very margins of the ice sheets. Anything less than three iterations is suitable only for schematic purposes.

The marked discrepancy between velocity field VF1 [*Argus et al.*, 2014] and the *CALSEA*-derived VF2 across the ice shelves suggests that one of the two sets of calculations is mishandling the change in load across these regions. To determine which of the two calculations might be in error, we investigated the two regions marked in Figure 4. Region A covers the longitude range 291–303°E and latitude range 82–78°S (this is the region of maximum uplift in the VF1 model) while region B is defined by longitude range 230–242°E, latitude range 81–85°S (this is the region of maximum change in ice thickness in the *ICE6G_C* model). The average topography values across regions A and B derived from the topographic data set used by *CALSEA* are −403 m and 951 m, respectively. In both regions, *ICE6G_C* average ice thickness starts out well above modern values (+747 m for region A, +1233 m for region B) at 26 ka B.P. and remains stable until 12 ka B.P. before declining to modern values by 4 ka B.P. Using the analytical expressions derived above, the net change in load for region A would be

$$\begin{aligned}\rho_w b(\text{present}) - \rho_i I(-12) &= 1027 \times 403 - 893 \times 747 \\ &= -0.253 \times 10^6\ \text{kg m}^{-2}\end{aligned}$$

assuming that the ice load was initially grounded (since global sea level was lower at the LGM). For region B the corresponding change in load would be

$$\begin{aligned}\rho_i I(\text{present}) - \rho_i I(-12) &= 893 \times -1233 \\ &= -1.10 \times 10^6\ \text{kg m}^{-2}\end{aligned}$$

From this analysis we see that in broad terms, the total change in load is roughly 4 times larger for region B than it is for region A.

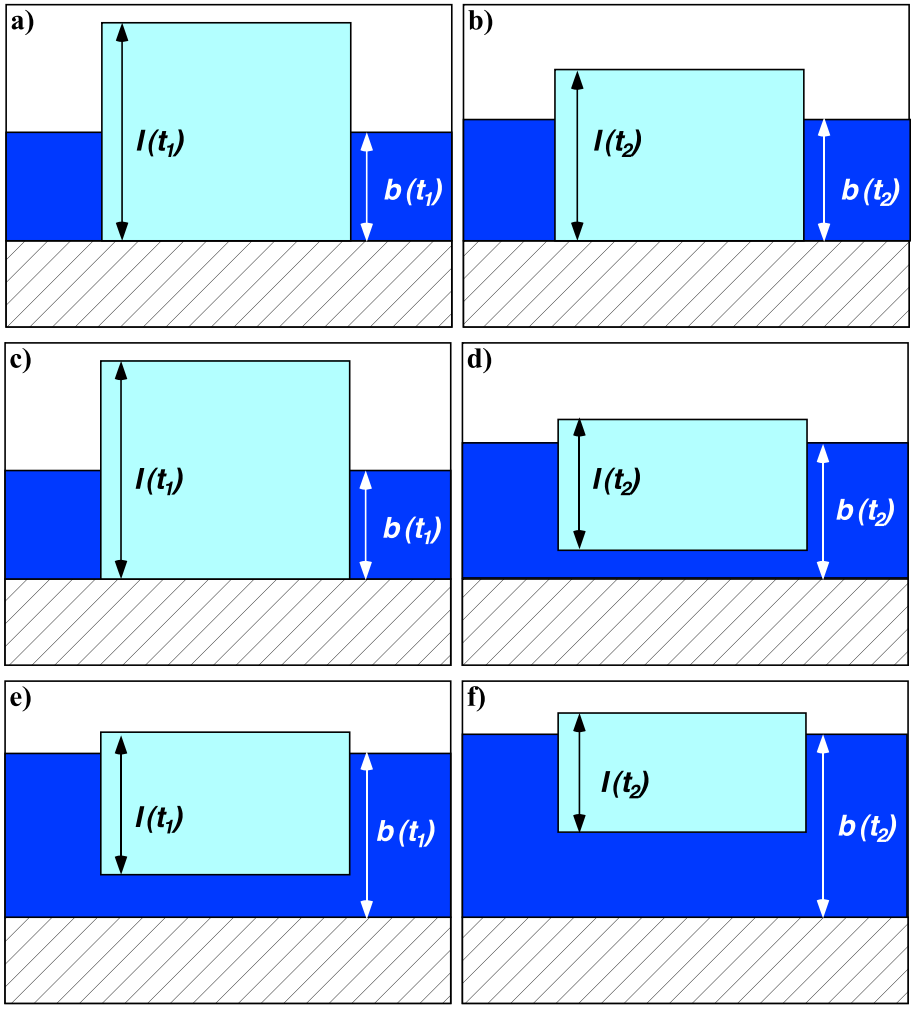

Figure 3. Illustration of potential surface load changes due to a reduction in ice thickness. (a, c, and e) Initial configuration (ice thickness $l(t_1)$, water depth $b(t_1)$); (b, d, and f) final configuration (ice thickness $l(t_2)$, water depth $b(t_2)$). In Figures 3a and 3b the ice sheet is grounded at both time steps ($\rho_i l(t) > \rho_w b(t)$) and the change in load beneath the ice sheet is $\rho_i(l(t_2) - l(t_1))$. This condition holds trivially at all points above contemporary sea level where $l(t) \geq 0$ and $b(t) = 0$. In Figures 3c and 3d the ice sheet is initially grounded but thins to the point that it floats ($\rho_i l(t_1) > \rho_w b(t_1)$, $\rho_i l(t_2) < \rho_w b(t_2)$) and the net change in load beneath the ice sheet is $\rho_w b(t_2) - \rho_i l(t_1)$. Figures 3e and 3f show the case where the ice sheet is at no point grounded ($\rho_i l(t) < \rho_w b(t)$) and the change in load is simply the change in water depth $\rho_w(b(t_2) - b(t_1))$. This is trivially the case for all points where $l(t) = 0$ and $b(t) > 0$.

For the velocity field of *Argus et al.* [2014] and *Peltier et al.* [2015] (VF1) region A has an average velocity of 10.34 mm/yr, while region B has an average uplift rate of 9.36 mm/yr. For the *CALSEA*-derived velocity field (VF2) region A has an average uplift rate of 4.37 mm/yr and region B has an average uplift rate of 10.5 mm/yr. While there is reasonable agreement between the two velocity fields over region B, there is a stark divergence over region A. For the *CALSEA*-derived velocity field VF2 the uplift rates are broadly consistent with the load over region A being 4 times smaller than for region B but for VF1 the predicted uplift for region A is 15% larger than for region B. Given that the change in load in region A is substantially smaller than that in region B, it is difficult to see how this result is consistent with the physics of the system. That this problem occurs at a location where there is a transition from ice loading to water loading is significant, suggesting that for whatever reason, the net change in load is not being correctly calculated in the analysis of *Peltier et al.* [2015] and *Argus et al.* [2014].

The agreement between VF1 and VF2 over region B suggests broad compatibility in the Love number formulation between the *CALSEA* code and the formalism of *Peltier et al.* [2015]. If there were some systematic discrepancy between the two Love number calculations in the Laplace domain or the inversion to the time

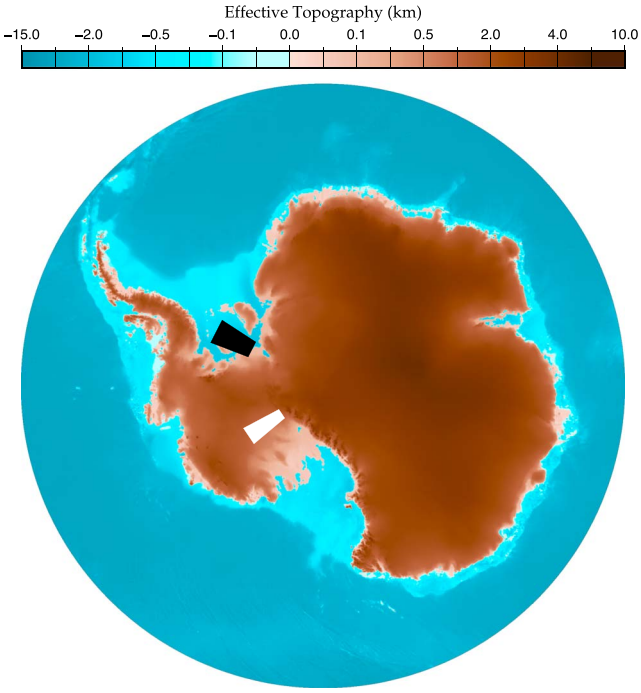

Figure 4. Illustration of the topographic data set used by the *CALSEA* software package. The Antarctic component of the data set is derived from BEDMAP-2 with ice elevation substituting for topography where the modern ice sheet is grounded. The data set is defined at a grid resolution of 1 min in latitude and longitude. The two areas across which the *ICE6G_C* velocity values are analyzed are shown as shaded sectors, region A (291–303°E, 82–78°S) is in black and region B (230–242°E, 81–85°S) is in white.

domain, this would manifest itself in systematic discrepancies for particular harmonic degrees. The generally small differences shown in Figure 1 are not consistent with such an explanation. The geographic coherence of the difference between the two fields and its marked correlation with regions where ice-water transitions occur strongly suggests that the cause of the difference lies in the load calculation and not in the Earth response calculation.

It must be emphasized that the above discussion of regional averages is vastly simplified, a crude analysis of this sort is inherently less than rigorous and should not be used as anything other than a rough guide to the order of magnitude of the various effects. Such a calculation neglects the specific change in load distribution in space and time, and the effects of neighboring ice and water loads. Nonetheless, this simple analysis provides a useful diagnostic test against which the numerical results may be compared. Even given the limitations discussed above, it is apparent that the *Peltier et al.* [2015] and *Argus et al.* [2014] results for the Antarctic near field are physically implausible and, consequently, the results presented in both papers contain a substantial methodological error.

The transition from ice loading to water loading is discussed in detail in *Mitrovica and Milne* [2003] and *Lambeck et al.* [2003], with the two papers using very similar algorithms. *Peltier* [1998] introduced a very different approach that has so far not been independently replicated but gives quite distinct values for the postglacial water loading effect. It is beyond the scope of the current paper to explore why the radial uplift field given by *Peltier et al.* [2015] and *Argus et al.* [2014] is inconsistent with the load history. Nonetheless, the fact that it is inconsistent makes the velocity fields, gravitational changes, and RSL estimates of *Peltier et al.* [2015] and *Argus et al.* [2014] subject to significant error, particularly in the Antarctic near field but more generally in any region where an ice load to water load transition has occurred (such as the Hudson Bay, Baffin Bay, and the Baltic Sea) or where paleotopography has transitioned from below sea level to above (which is the case for much of Canada).

3.2. Spherical Harmonic Representation of *ICE6G_C(VM5a)*

Peltier et al. [2015] provided a spherical harmonic representation of the present-day glacial isostatic response of the Earth as predicted by their model. In principle, this can be used to remove the effects of GIA from

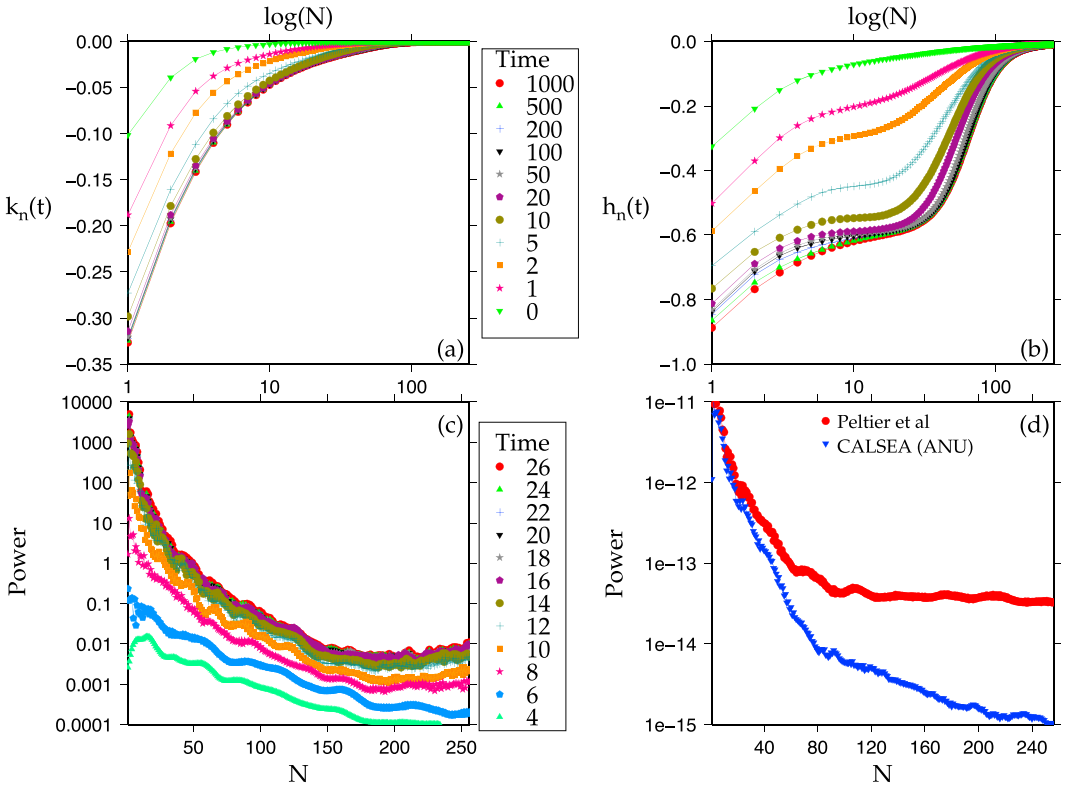

Figure 5. Analysis of power spectrum and response functions. (a) Comparison of normalized gravitational Love numbers (k_n) for Earth model VM5 as a function of time. Time units are kiloannum. (b) Comparison of normalized radial deformation Love numbers (h_n) for Earth model VM5 as a function of time. It should be noted that the values of h_n are of greater magnitude and decay more slowly than those of k_n and that this trend becomes more pronounced at higher degree. (c) Power spectrum of *ICE6G_C* from 26 ka B.P. to the end of melting at 4 ka B.P. (d) Power spectrum of the Stokes' coefficients for *ICE6G_C(VM5a)* given by *Peltier et al.* [2015] (red) and the *CALSEA*-derived spherical harmonic representation of *ICE6G_C(VM5a)* (blue).

space gravity estimates of the Earth's temporal gravity field so that present-day mass balance changes can be determined. It can also be used to correct satellite altimetry for GIA to yield estimates of present-day sea level variations. The spherical harmonic rate model, to degree and order 256, was provided by *Peltier et al.* [2015] as dimensionless Stokes' coefficients in their supporting information.

Peltier et al. [2015] and *Argus et al.* [2014] also evaluated the accuracy with which the empirical relation of *Purcell et al.* [2011] can reproduce GIA uplift rates derived from their rigorous computation using a full ice/Earth model to solve the sea level equation. Their computed differences between the empirical and full computations of present-day uplift rates showed strikingly large, high-frequency spatial errors when evaluated to degree 256 (see their Figures S2–S4), which prompted us to investigate further the power spectrum of their spherical harmonic model (Figure 5d). For degrees greater than 100 the deformational and gravitational effects of the load are relatively small (as shown in Figures 5a and 5b). For these shorter wavelengths the power spectrum of the ice sheet is several orders of magnitude smaller than for the low-degree terms and what power there is decays with time (Figure 5c). Consequently, the convolution of the load and the viscoelastic Love numbers should diminish at high degrees. However, the coefficients provided by *Peltier et al.* [2015] do not display this pattern, with very similar power found in coefficients of all degrees from ~60 onward.

We used the provided coefficients and the empirical relation of *Purcell et al.* [2011] to try to replicate the difference in uplift rate over Antarctica shown in *Peltier et al.* [2015, Figure S4]. We compared our computed uplift rates to the available gridded values (http://www.atmosp.physics.utoronto.ca/~peltier/data) and found a similar difference (compare our Figure 6a with their Figure S4e). However, to generate this, we had to use the empirical, linear formula of *Purcell et al.* [2011] (their equation (3)) for all degrees, whereas *Purcell et al.* [2011] stated that for degrees >60, their tabulated values should be used to represent the ratio of the h_n^{ve}/k_n^{ve} Love numbers (a significant nonlinearity in the ratios becomes apparent and quite significant for degrees >60 as

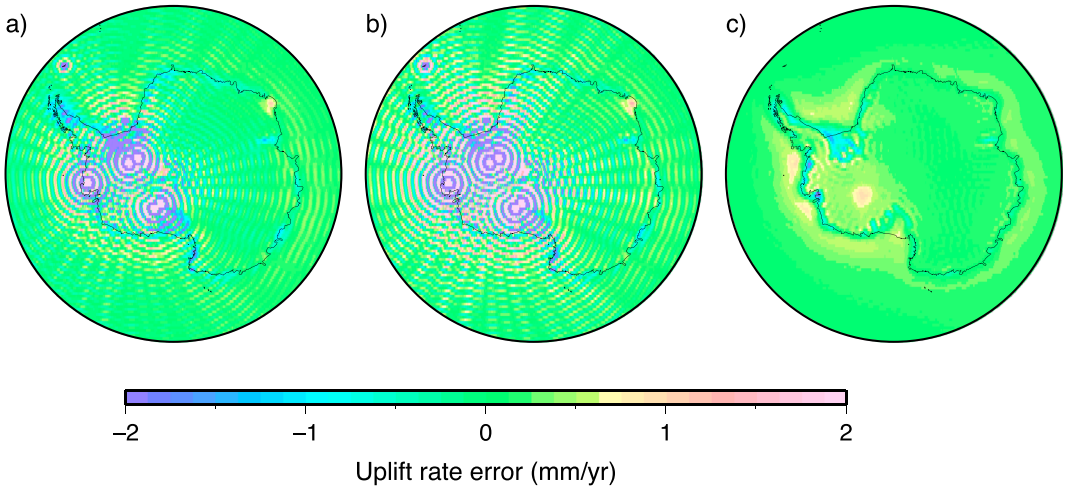

Figure 6. Difference in uplift rates between those computed in a fully rigorous manner by *Peltier et al.* [2015] and the degree 256 spherical harmonic model of *Peltier et al.* [2015] using (a) the linear relation of *Purcell et al.* [2011] and (b) the nonlinear, tabulated values of *Purcell et al.* [2011]. (c) Difference between our fully rigorous computation of radial uplift for *ICE6G_C(VM5a)* and our degree 256 Stokes' coefficient representation of it, using the nonlinear tabulated values of *Purcell et al.* [2011]. Note that the maximum error in Figure 6c is <1 mm/yr over the continent (excluding the ice shelves where water loads have changed in the past 6000 years).

shown in *Purcell et al.* [2011, Figure 3a]). This is a relatively minor oversight if, as in *Purcell et al.* [2011], one were to focus on the application of their method to GRACE observations which consist of relatively low-degree terms. However, when we correctly applied their empirical relation, we found that the differences in computed uplift rates actually increased compared to the rates from the fully rigorous computation (Figure 60b).

Next, we derived uplift rates from our own fully rigorous computation of the *ICE6G_C* ice history (see section 3.1 above), along with a spherical harmonic representation of the corresponding change in gravity. We calculated the differences between these uplift rates and uplift velocities that we obtained by processing the *CALSEA*-derived Stokes' coefficients with the correct empirical relation of *Purcell et al.* [2011]. This procedure produces significantly smaller differences than in the previous two cases (Figure 6c). This is in stark contrast to the conclusion of *Peltier et al.* [2015] who stated "It is in this region that the errors in the prediction using the formula of *Purcell et al.* [2011] are especially large, so large as to apparently render the formula inapplicable for the prediction of vertical motion of the crust on the basis of the geoid Stokes' coefficients."

In fact, with the exception of regions beneath the floating ice shelves, the maximum error in Antarctica is <1 mm/yr. This confirms the validity of the empirical relation subject to the caveat stated by *Purcell et al.* [2011] that no significant load variation could have occurred in the past 6000 years for the empirical relation to be validly applied.

3.3. Reevaluation of Empirical Approximation for Uplift Rates Derived From Stokes' Coefficients

As shown in section 3.2, the correct use of the empirical relation of *Purcell et al.* [2011] enables viscoelastic uplift rates to be derived with an error <1 mm/yr over continental Antarctica. The caveat on the use of this empirical approximation is that there cannot have been changes in the load in the past 6000 years; otherwise, the approximation becomes invalid because the Love number ratios will not have had time to reach stable values that permit the empirical relation to be applied (as shown in *Purcell et al.* [2011, Figure 2]).

What is the magnitude of the error in the technique when applied in regions where loads have continued to change in the past 6000 years? To evaluate this, we consider the region of the North American Ice Sheet complex in Canada. In the *ICE6G_C* model, the ice sheets in this region had essentially melted by 6000 years ago, so one would expect the empirical approximation to be valid. Figure 7a shows the difference between the fully rigorous computations of present-day uplift rates and those using the empirical approximation evaluated to degree 256. As we saw in the case of Antarctica, the maximum error over land is <1 mm/yr; however, there are markedly larger errors clearly visible in regions where the water load has changed significantly. In particular, the velocity errors in Hudson Bay reach -4 mm/yr. There are also positive errors visible in the Labrador Sea, Baffin Bay, along the northern coast of Canada, and even on the west coast of North America and south

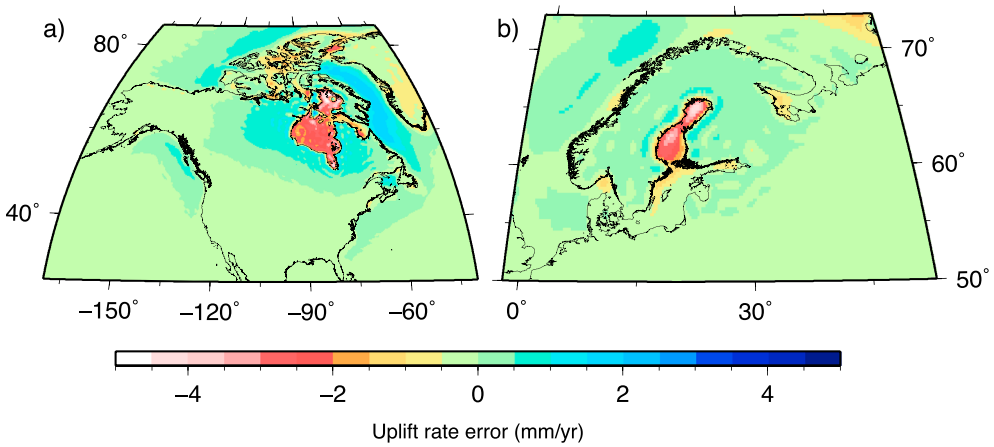

Figure 7. Difference in uplift rates between those computed in a fully rigorous manner and from our degree 256 spherical harmonic model using the empirical relation of *Purcell et al.* [2011]. (a) Laurentide region; (b) Fennoscandia. Errors are typically <1 mm/yr over land and can reach several mm/yr in ocean regions that have experienced significant changes in water depth due to GIA uplift or peripheral bulge subsidence changing the water loads in the past 6000 years.

of Nova Scotia. These differences are due to large amplitude changes in water depth that have continued to occur in the oceans long after the ice sheet had disappeared. A similar effect is seen in the Baltic Sea in the region of the Fennoscandian Ice Sheet (Figure 7b).

Due to the ongoing effects of GIA the sea floor of Hudson Bay has been uplifting at a rate of 3–10 mm/yr, resulting in a reduction in water depth within the bay of tens of meters in the last 6000 years. Thus, the water load has decreased significantly (by approximately 50% of the current water depth within the bay) during this period. Consequently, it is invalid to apply the empirical relation of *Purcell et al.* [2011] over this area. Similarly, the regions of positive error around the coastal margins of the former North American ice sheet complex all occur in locations where the peripheral bulge is subsiding and the water load is consequently increasing (there may also be some signal related to the peripheral bulge of the Greenland Ice Sheet). The "peripheral bulge" of an ice sheet is the region that uplifted as the ice load increases to accommodate lithospheric flexure and the flow of mantle material from beneath the ice sheet. Conversely, when the ice sheet melts, the mantle material flows back under the formerly glaciated region, causing subsidence of the peripheral bulge. Thus, in regions where the peripheral bulge coincides with a nonzero water load, ocean depth increases as the peripheral bulge subsides which causes a corresponding increase in the water load. Again, this process persists through the last 6000 years and invalidates the use of the *Purcell et al.* [2011] approximation in these oceanic regions. It is notable how exactly the error induced by the empirical relation follows the modern coastline in these regions.

Nonetheless, we confirm that the empirical relation using our degree 256 spherical harmonic representation of the *ICE6G_C* ice history and the tabulated Love number ratio values of *Purcell et al.* [2011] is able to reproduce—to within 1 mm/yr—the fully rigorous computation of uplift rates for continental regions that have not seen any significant change in ice load in the past 6000 years. However, reducing the maximum degree significantly degrades the quality of the agreement, and it is recommended that the full series to degree 256 be applied wherever possible.

4. Conclusions

Our assessment of the *ICE6G_C(VM5a)* model of *Argus et al.* [2014] and *Peltier et al.* [2015] has raised three important issues. First, we found significant differences in uplift rate between published values and our own computations in regions where paleotopography had transitioned from lying below sea level to lying above and vice versa. This misfit is particularly large in the Weddell and Ross Seas in the near-field region of the Antarctic Ice Sheet. A broad-scale assessment of net load change in the Weddell Sea and the Ohio Mountains, Antarctica, shows that the radial uplift rate over the Weddell Sea given in the *Argus et al.* [2014] and

Peltier et al. [2015] studies does not represent well the change in surface load for this area, whereas our derived velocity field agrees with the physical characteristics of the system. We denote our present-day radial velocity field *ICE6G_ANU* and provide a global-coverage gridded data set in Data Set S1 in the supporting information.

Second, the Stokes' coefficients describing the modern change in geoid elevation given by *Argus et al.* [2014] and *Peltier et al.* [2015] do not describe the present-day GIA signal of the *ICE6G_C(VM5a)* model itself. The power spectrum of the coefficients provided by *Peltier et al.* [2015] has power at high degrees that is 2 orders of magnitude greater than the power of our computed coefficients, and the power of the former does not decrease substantially for degrees >90. Again, this does not accord with the expected physics of the system where the response should become nearly elastic as degree increases and load wavelength decreases. The error in their published spherical harmonic coefficients (mis)led *Argus et al.* [2014] and *Peltier et al.* [2015] to conclude that there was an error in the empirical formula of *Purcell et al.* [2011].

Third, when we apply the empirical formula of *Purcell et al.* [2011] to our derived Stokes' coefficients for *ICE6G_ANU*, we obtain an uplift rate field that agrees very closely with the rigorously calculated velocity field. We thus confirm the validity of the empirical relationship derived by *Purcell et al.* [2011]. We have verified that the technique is accurate when applied to the *ICE6G_C* ice history using the VM5a rheology model, generating uplift rates within 1 mm/yr of fully rigorous computations for regions where there has been no significant change in load over the last 6000 years, as originally noted by *Purcell et al.* [2011]. We provide the *ICE6G_ANU* Stokes' coefficients in Data Set S2 in the supporting information.

The *ICE6G_C* ice history model was derived by *Argus et al.* [2014] and *Peltier et al.* [2015] by inverting a global data set of geodetic and geological observations. Their inversions rely implicitly on the accuracy of the forward modeling procedure employed. The results of this study demonstrate that some of the algorithms they used seem to misrepresent the net change in ice/water loads in the near field. Following the submission of this manuscript, a new release of the *ICE6G_C(VM5a)* spherical harmonic coefficients became available on the Toronto group's website. In this new spherical harmonic expansion the strange high-frequency pattern shown in Figures 6a and 6b has been removed. We note, however, that the anomalously large uplift signals in regions of ice-marine transitions remains in the new formulation. These are caused by the water loading algorithm used by *Peltier et al.* [2015] and *Argus et al.* [2014] to compute the *ICE6G_C(VM5a)* model. Assessing the validity of the resulting ice sheet reconstructions in light of this issue is beyond the scope of this study.

Acknowledgments

We thank W.R. Peltier for making the ice thickness history and gridded uplift rate values available for the *ICE6G_C(VM5a)* model and J.X. Mitrovica for providing rotational correction terms for *ICE6G_C(VM5a)*. Figures were plotted using GMT *Wessell and Smith* [1998]. Calculations were performed on the Terrawulf cluster, a computational facility supported through the AuScope initiative. AuScope Ltd. is funded under the National Collaborative Research Infrastructure Strategy (NCRIS), an Australian Commonwealth Government Programme. We would also like to thank the two anonymous reviewers of this article for their constructive suggestions on its improvement. The data for this paper are available by contacting the corresponding author at anthony.purcell@anu.edu.au.

References

Argus, D. F., W. R. Peltier, Drummond R., and A. W. Moore (2014), The Antarctica component of postglacial rebound model ICE6G_C(VM5a) based upon GPS positioning, exposure age dating of ice thicknesses, and relative sea level histories, *Geophys. J. Int.*, *198*(1), 537–563, doi:10.1093/gji/ggu140.

Cambiotti, G., and R. Sabadini (2010), The compressional and compositional stratifications in Maxwell Earth models: The gravitational overturning and the long-period tangential flux, *Geophys. J. Int.*, *180*, 475–500.

Dal Forno, G., P. Gasperini, and E. Boschi (2005), Linear or nonlinear rheology in the mantle: A 3D finite-element approach to postglacial rebound modeling, *J. Geodyn.*, *39*(2), 183–195.

Dziewonski, A. M., and D. L. Anderson (1981), Preliminary reference Earth model, *Phys. Earth Planet. Int.*, *25*, 297–356.

Farrell, W. E., and J. A. Clark (1976), On postglacial sea level, *Geophys. J. R. Astron. Soc.*, *46*, 647–667.

Fretwell, L. O., et al. (2013), Bedmap2: Improved ice bed, surface and thickness datasets for Antarctica, *The Cryosphere*, *7*, 375–393.

Johnston, P. (1993), The effect of spatially non-uniform water loads on predictions of sea level change, *Geophys. J. Int.*, *114*, 615–634.

Kendall, R. A., J. X. Mitrovica, and G. A. Milne (2004), On post-glacial sea level II. Numerical formulation and comparative results on spherically symmetric models, *Geophys. J. Int.*, *161*, 679–706, doi:10.1111/j.1365-246X.2005.02553.x.

Lambeck, K. (1980), *The Earth's Variable Rotation: Geophysical Causes and Consequences*, Cambridge Univ. Press, London.

Lambeck, K., and A. Purcell (2005), Sea-level change in the Mediterranean Sea since the LGM: Model predictions for tectonically stable areas, *Quat. Sci. Rev.*, *24*, 1969–1988.

Lambeck, K., C. Smither, and P. Johnston (1998), Sea-level change, glacial rebound and mantle viscosity for northern Europe, *Geophys. J. Int.*, *134*, 102–144.

Lambeck, K., A. Purcell, P. Johnston, M. Nakada, and Y. Yokoyama (2003), Water-load definition in the glacio-hydro-isostatic sea-level equation, *Quat. Sci. Rev.*, *22*, 309–318.

Lambeck, K., A. Purcell, S. Funder, K. K.Kjær, E. Larsen, and P. Möller (2006), Constraints on the Late Saalian to early Middle Weichselian ice sheet of Eurasia from field data and rebound modelling, *Boreas*, *35*(3), 539–575.

Lambeck, K., A. Purcell, J. Zhao, and N-O Svensson (2010), The Scandinavian ice sheet: From MIS 4 to the end of the Last Glacial Maximum, *Boreas*, *39*(2), 410–435, doi:10.1111/j.1502-3885.2010.00140.x.

Lambeck, K., H. Rouby, A. Purcell, Y. Sun, and M. Sambridge (2014), Sea level and global ice volumes from the Last Glacial Maximum to the Holocene, *Proc. Nat. Acad. Sci.*, *111*(43), 15,296–15,303, doi:10.1073/pnas.1411762111.

Milne, G. A. (1998), Refining models of the glacial isostatic adjustment process, PhD thesis, Univ. of Toronto, Toronto.

Milne, G. A., and J. X. Mitrovica (1998), Postglacial sea level change on a rotating Earth, *Geophys. J. Int.*, *133*, 1–10.

Mitrovica, J. X. (2003), Recent controversies in predicting post-glacial sea-level change: A viewpoint, *Quat. Sci. Rev.*, *22*, 127–133.

Mitrovica, J. X., and G. A. Milne (2003), On post-glacial sea level: I. General theory, *Geophys. J. Int.*, *154*(2), 253–267, doi:10.1046/j.1365-246X.2003.01942.x.

Mitrovica, J. X., and W. R. Peltier (1991), A comparison of methods for the inversion of viscoelastic relaxation spectra, *Geophys. J. Int.*, *108*, 410–414.
Mitrovica, J. X., and J. Wahr (2011), Ice age Earth rotation, *Ann. Rev. Earth Planet. Sci.*, *39*, 577–616, doi:10.1146/annurev-earth-040610-133404.
Mitrovica, J. X., J. Wahr, I. Matsuyama, and A. Paulson (2005), The rotational stability of an ice-age Earth, *Geophys. J. Int.*, *161*, 491–506.
Mound, J. E., J. X. Mitrovica, and A. M. Forte (2003), The equilibrium form of a rotating earth with an elastic shell, *Geophys. J. Int.*, *152*, 237–241.
Nakada, M., and K. Lambeck (1987), Glacial rebound and relative sea-level variations: A new appraisal, *Geophys. J. R. Astron. Soc.*, *90*, 171–224.
Nakada, M., and K. Lambeck (1989), Late Pleistocene and Holocene sea-level change in the Australian region and mantle rheology, *Geophys. J. Int.*, *96*, 497–517.
Paulson, A., and M. A. Richards (2009), On the resolution of radial viscosity structure in modelling long-wavelength postglacial rebound data, *Geophys. J. Int.*, *179*(3), 1516–1526, doi:10.1111/j.1365-246X.2009.04362.x.
Paulson, A., S. Zhong, and J. Wahr (2005), Modelling post-glacial rebound with lateral viscosity variations, *Geophys. J. Int.*, *163*(1), 357–371, doi:10.1111/j.1365-246X.2005.02645.x.
Paulson, A., S. Zhong, and J. Wahr (2007), Limitations on the inversion for mantle viscosity from postglacial rebound, *Geophys. J. Int.*, *168*(3), 1195–1209, doi:10.1111/j.1365-246X.2006.03222.x.
Peltier, W. R. (1994), Ice age paleotopography, *Science*, *265*, 195–201.
Peltier, W. R. (1998), Implicit ice in the global theory of glacial isostatic adjustment, *Geophys. Res. Lett.*, *25*, 3955–3958.
Peltier, W. R. (2004), Global glacial isostasy and the surface of the ice-age Earth: The ICE-5G (VM2) model and GRACE, *Ann. Rev. Earth Planet. Sci.*, *32*, 111–149.
Peltier, W. R., D. F. Argus, and R. Drummond (2015), Space geodesy constrains ice-age terminal deglaciation: The global ICE6G_C(VM5a) model, *J. Geophys. Res. Solid Earth*, *120*, 450–487, doi:10.1002/2014JB011176.
Purcell, A., A. Dehecq, P. Tregoning, K. Lambeck, E.-K. Potter, and S. McClusky (2011), Relationship between the Glacial Isostatic Adjustment and gravity perturbation observed by GRACE, *Geophys. Res. Lett.*, *38*, L18305, doi:10.1029/2011GL048624.
Sabadini, R., and W. R. Peltier (1981), Pleistocene deglaciation and the Earth's rotation: Implications for mantle viscosity, *Geophys. J. R. Astron. Soc.*, *66*, 553–578.
Tushingham, A. M., and W. R. Peltier (1992), Validation of the ICE-3G model of Würm-Wisconsin deglaciation using a global data base of relative sea level histories, *J. Geophys. Res.*, *97*, 3285–3304.
Wessel, P., and W. H. F. Smith (1998), New, improved version of the Generic Mapping Tools released, *Eos Trans. AGU*, *79*, 579.
Wu, P., and W. R. Peltier (1982), Viscous gravitational relaxation, *Geophys. J. R. Astron. Soc.*, *70*, 435–485.
Wu, P., and W. R. Peltier (1984), Pleistocene deglaciation and the Earth's rotation: A new analysis, *Geophys. J. R. Astron. Soc.*, *76*, 753–792.
Wu, P., and W. Van Der Wal (2003), Postglacial sea levels on a spherical, self-gravitating viscoelastic Earth: Effects oflateral viscosity variations in the upper mantle on the inference of viscosity contrasts in the lower mantle, *Earth Planet. Sci Lett.*, *211*, 57–68.
Yuen, D. A., R. Sabadini, and E. Boschi (1982), Viscosity of the lower mantle as inferred from rotational data, *J. Geophys. Res.*, *87*, 10,745–10,762.